Quantum Clusters of Gold Exhibiting FRET

M. A. Habeeb Muhammed,[†] Ajay Kumar Shaw,[‡] Samir Kumar Pal,*[,‡] and T. Pradeep*[,†]

DST Unit on Nanoscience, Department of Chemistry and Sophisticated Analytical Instrument Facility, Indian Institute of Technology Madras, Chennai 600 036, India, and Unit for Nanoscience and Technology, Department of Chemical, Biological and Macromolecular Sciences, Satyendra Nath Bose National Centre for Basic Sciences, Block JD, Sector III, Salt Lake, Kolkata 700 098, India

Received: May 24, 2008; Revised Manuscript Received: June 25, 2008

Fluorescence resonance energy transfer between the metal core and the ligand in $Au_{25}SG_{18}$ (SG-glutathione thiolate) is demonstrated using dansyl chromophores attached to the cluster core through glutathione linkers. The dansyl chromophore functionalization of the cluster has been carried out by two different routes. Efficient energy transfer from the dansyl donor to the Au_{25} core is manifested by way of the reduced lifetime of the excited state of the former and drastic quenching of its fluorescence. The donor−acceptor separation observed in the two synthetic routes reflects the asymmetry in the ligand binding on the cluster core, which is in agreement with the recent theoretical and experimental results on the structure of Au_{25}.

1. Introduction

Fluorescence resonance energy transfer (FRET) is an ideal tool to measure the separation between an excited donor (D) and an acceptor (A) as the extent of such dipole interactions is a sensitive measure of the D−A distance. This technique is widely used for studying the structural dynamics of biomolecules. From single-molecule protein folding[1] to detection of DNA cleavage,[2] the applications of FRET have been many and have been increasing rapidly recently. Compared with conventional chemical analysis, FRET-based analytical methods have higher sensitivity and greater simplicity for detection of ligand−receptor binding by observing merely the enhanced fluorescence of the acceptor.[3] Increasing the Förster distance of energy transfer by metal-enhanced FRET[4] can increase the scope of this tool.

A review of the literature on the use of nanoparticles in FRET applications gives several interesting papers. FRET-based applications include sensing, imaging, detection, therapy, and monitoring structural changes of biomolecules. Since semiconductor nanoparticles or quantum dots are strongly fluorescent, they are widely used in FRET-based techniques.[5−14] CdSe/ZnS quantum dot-aptamer conjugates are used in targeted cancer imaging, sensing, and therapy based on FRET.[5] Cds/ZnS quantum dots can be used as protease sensors by employing FRET.[6] One-dimensional aggregates of CdTe quantum dots show strong FRET between the particles, which is due to the migration of the excitation along the chain, similar to wave guiding of light observed for chains of metal nanoparticles.[7] Water-soluble, oppositely charged CdSe/ZnS core/shell quantum dots can be used as FRET-based sensors with a donor quenching efficiency close to 100%.[8] FRET-scanning near-field optical microscopy imaging can be carried out with a tip made from a single bead coated with CdTe.[9] Semiconductor nanocrystals are used to functionalize atomic force microscope (AFM) tips and can be used in FRET microscopy.[10] FRET from the amino acid, tryptophan, to CdS quantum dots functionalized with human serum albumin has been monitored to follow the local and global changes in the protein structure during thermal unfolding and refolding processes.[11] Metal nanoparticles, especially of gold, are also widely studied for FRET-based techniques.[15−24] A gold-nanoparticle-based FRET probe has been developed for ultrasensitive detection of anthrax DNA.[15] In a recent report, a rapid and simple immunoassay protocol for detection of C-reactive protein and osteopontin has been developed by mixing them with gold nanoparticles and employing FRET between them.[16] An inhibition assay method was developed based on the modulation in FRET between quantum dots and gold nanoparticles in the presence of molecules which inhibit the interactions between them.[17] A gold-nanoparticle-based miniaturized nanomaterial surface energy-transfer probe has been developed recently for the rapid and ultrasensitive detection of mercury in soil, water, and fish.[18] Fluorescent lifetime quenching near a gold nanoparticle of 1.5 nm diameter has been demonstrated.[19] Enhanced sensitized near-infrared (NIR) luminescence from gold nanoparticles was observed via energy transfer from surface-bound fluorophores.[20] Nanoparticle-induced lifetime modification has promise in serving as a nanoscopic ruler for the distance range well beyond 10 nm.[21] DNA sequence can be detected using selective fluorescence quenching of tagged oligonucleotide probes by gold nanoparticles.[22] Several other materials such as polymeric nanoparticles have also been used in FRET applications.[25−27] Optically switchable dual-color fluorescent PNIPAM nanoparticles that incorporate two classes of dyes into polymeric chains were developed as a potential tool for biomedical applications and live-cell imaging.[25] A new pH-sensitive polymeric sensor with a donor molecule at one end and an acceptor molecule at the other end has been synthesized, and its pH sensitivity has been examined on the basis of FRET efficiency.[26] Spatial organization of polymer chains upon ionic or covalent cross-linking to form a hydrogel has been examined on the molecular scale using FRET.[27]

Recently, a new class of compounds of gold called quantum clusters has been synthesized.[28−38] They are characterized in terms of the number of gold atoms in the core such as Au_8, Au_{11}, Au_{13}, Au_{25}, etc., rather than the core diameter. They are extremely small and cannot be seen clearly in the transmission

* Corresponding authors. Fax: + 91-44 2257-0545. E-mail: skpal@bose.res.in and pradeep@iitm.ac.in.
[†] Indian Institute of Technology Madras.
[‡] Satyendra Nath Bose National Centre for Basic Sciences.

10.1021/jp804597r CCC: $40.75 © 2008 American Chemical Society
Published on Web 08/21/2008

electron microscope. Their chemical composition such as the number of core atoms and number of protecting ligands is deduced using mass spectroscopic techniques.[33,34] Due to the very small size (~1 nm), they exhibit molecular transitions in absorption and emission and are totally different from the conventional metallic nanoparticles possessing surface plasmon resonance, and different synthetic approaches have been followed to make them. Because of the strong quantum size effect, quantum clusters possess characteristic absorption and emission profiles due to intraband and interband transitions[33,39] and can be distinguished from each other very easily from these features. Glutathione (GSH) protected gold quantum clusters[32−37] (Au_n-SG_m) (-SG, glutathione thiolate) is one such group of compounds which have been well known for some years. Glutathione is a tripeptide consisting of three amino acids, namely, glutamic acid, cysteine, and glycine. Out of the various glutathione-protected clusters such as $Au_{10}SG_{10}$, $Au_{15}SG_{13}$, $Au_{18}SG_{14}$, $Au_{22}SG_{16}$, $Au_{22}SG_{17}$, $Au_{25}SG_{18}$, $Au_{29}SG_{20}$, $Au_{33}SG_{22}$, and $Au_{39}SG_{24}$, $Au_{25}SG_{18}$ is the most thermodynamically stable one. The bigger clusters, $n > 25$, can be converted into $Au_{25}SG_{18}$ by adding excess glutathione. This extra stability of $Au_{25}SG_{18}$ arises due to the chemical inertness by the complete coverage of the gold core by glutathione ligands.[35] With the availability of these fluorescent molecular gold clusters, application of them in FRET becomes a distinct possibility. There has been no report to date using quantum clusters of gold in FRET. There have not been many applications of such quantum clusters till recently, particularly due to their unavailability in sufficiently large quantities. Various methods have been developed recently[34−38] to synthesize molecular clusters in gram quantities. Here we present the first report of the observation of FRET between the dansyl group (D) and the molecular cluster, Au_{25} (A), linked through glutathione. Efficient nonradiative transfer of energy from D to A occurs in femtosecond time scales.

2. Experimental Section

All chemicals were commercially available and used without further purification.

1. Synthesis of Glutathione-Capped Gold (Au@SG) Clusters. Glutathione-capped gold clusters were synthesized according to a reported method.[33] To 100 mL of 5 mM $HAuCl_4 \cdot 3H_2O$ in methanol, 20 mM reduced glutathione (GSH) was added. The mixture was then cooled to 0 °C in an ice bath for 30 min. An aqueous solution of $NaBH_4$ (25 mL, 0.2 M), cooled at 0 °C, was injected rapidly into this mixture under vigorous stirring. The mixture was allowed to react for another hour. The resulting precipitate was collected and washed repeatedly with methanol through centrifugal precipitation and dried to obtain Au@SG clusters as a dark brown powder. This product is a mixture of small nanoparticles and different clusters.

2. Synthesis of $Au_{25}SG_{18}$. $Au_{25}SG_{18}$ was synthesized from the as-prepared Au@SG clusters by ligand etching. The as-prepared Au@SG clusters were dissolved in 25 mL of water. GSH was added (20 mM) and stirred at 55 °C. The reaction was monitored by optical absorption spectroscopy. Heating was discontinued when the absorption features of $Au_{25}SG_{18}$ appeared in the UV−vis spectrum. This typically took 12 h of heating. The solution was centrifuged, and methanol was added to the supernatant to precipitate the cluster. The precipitate was dried to obtain $Au_{25}SG_{18}$ in the powder form. The prepared $Au_{25}SG_{18}$ shows characteristic UV−vis, FT-IR, and ^1H NMR features (Supporting Information 1).

3. Synthesis of Dansyl Glutathione (D-GSH).[40] A 140 mg amount of dansyl chloride (5-dimethylaminonaphthalene-1-sulfonyl chloride) in 2 mL of acetone was added dropwise to a solution of oxidized glutathione (150 mg) in aqueous NaOH (1.2 mL of a 1 M solution). The reaction mixture was allowed to stir for 30 min at room temperature. The mixture was then washed with diethyl ether twice, and the aqueous phase was lyophilized to give dansylated oxidized glutathione as a white powder. Nitrogen gas was bubbled into a solution of dansylated glutathione (285 mg) in 0.1 M Tris buffer (pH 8, 10 mL) for 10 min, after which dithiothreitol (DTT; 77 mg, 0.5 mmol) was added. The reaction mixture was stirred at room temperature for another 30 min under an atmosphere of N_2. The solution was adjusted to pH 4 with acetic acid and then lyophilized to give dansylated reduced glutathione. All experiments have been done with this reduced form. The synthesized dansyl glutathione is characterized by optical absorption and emission spectroscopy techniques and electrospray ionization (ESI-MS) (Supporting Information 2).

4. Functionalization of $Au_{25}SG_{18}$ with Dansyl Chromophore. Dansyl chromophore was attached to $Au_{25}SG_{18}$ by two routes.

(1) Direct Reaction of $Au_{25}SG_{18}$ with Dansyl Chloride. A 10 mg amount of $Au_{25}SG_{18}$ was dissolved in 5 mL of water. A 37 μL volume of NaOH was added, followed by 4.64 mg of dansyl chloride in 200 μL of acetone dropwise and stirred for 3 h. The product was precipitated by addition of methanol, centrifuged, washed three times with methanol and finally with ethanol, and dried to obtain a reddish brown powder.

(2) Exchange of Glutathione Ligands with Dansyl Glutathione. A 10 mg amount of $Au_{25}SG_{18}$ was stirred with 5.3 mg of synthesized dansylated reduced glutathione (D-GSH) for 3 h, and the product was precipitated by addition of methanol, centrifuged, washed three times with methanol and finally with ethanol, and dried to obtain a reddish brown powder.

Scheme 1 depicts the approaches used for functionalization of dansyl chromophore on Au_{25}. The products obtained after dansyl functionalization of $Au_{25}SG_{18}$ can be represented as $Au_{25}SG_{18-x}SGD_x$.

5. Details of Instrumentation. UV−vis spectra were measured with a Perkin-Elmer Lambda 25 instrument in the range of 200−1100 nm. Fourier transform infrared (FT-IR) spectra were measured with a Perkin-Elmer Spectrum One instrument. KBr crystals were used as the matrix for preparing the samples. High-resolution transmission electron microscopy of clusters was carried out with a JEOL 3010 instrument. The microscope was operated at 200 keV to reduce beam-induced damage of Au_{25} clusters. Nanoparticles were measured at 300 keV. The samples were drop casted on carbon-coated copper grids and allowed to dry in ambience. The Fourier transform nuclear magnetic resonance (FT-NMR) measurements were done with a JEOL 400 MHz instrument. The solvent used was D_2O. The electrospray ionization (ESI) mass spectrometric measurements were done with an MDX Sciex 3200 Q TRAP LC/MS/MS instrument in which the spray and extraction are orthogonal to each other. The samples taken in 1:1 water−methanol were electrosprayed at 5 kV. The spectra were averaged for 100 scans. Laser desorption ionization (LDI) mass spectrometric studies were conducted using a Voyager DE PRO Biospectrometry Workstation of Applied Biosystems MALDI-TOF MS. A pulsed nitrogen laser of 337 nm was used for the studies. Mass spectra were collected in positive-ion mode and averaged for 100 shots. Fluorescence measurements were carried out on a Cary Eclipse instrument. The band pass for excitation and emission was set as 5 nm. The experimentally obtained intensities in absorbance and emission as a function of wavelength, $I(W)$, have been

SCHEME 1: Approaches Used for Functionalization of Dansyl Chromophore on the Au_{25} Cluster

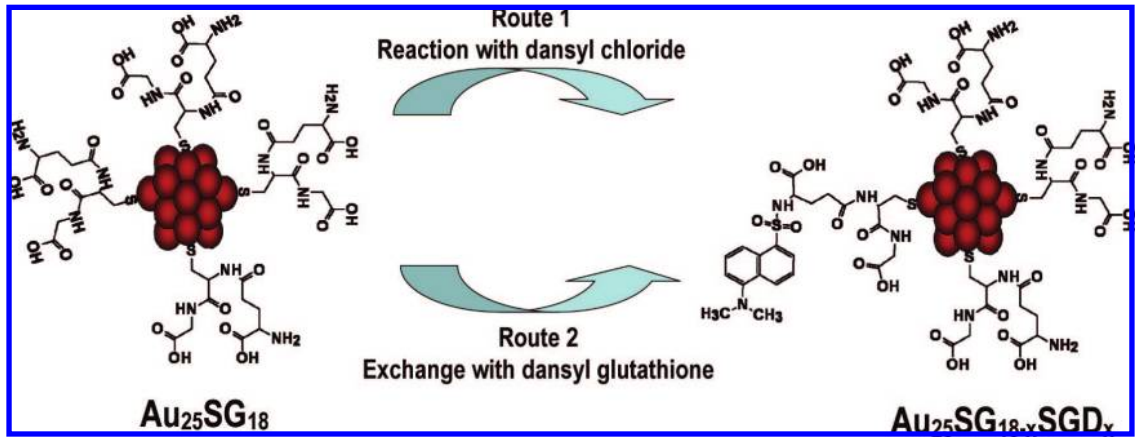

converted to energy-dependent values, $I(E)$, using the expression $I(E) = I(W)/(\partial E/\partial w) \alpha I(W) \times W^2$, where $\partial E/\partial w$ represents the Jacobian factor.

In our femtosecond upconversion setup (FOG 100, CDP) the sample was excited at 364 nm using the second harmonic of a mode-locked Ti-sapphire laser (Tsunami, Spectra Physics) pumped by 10 W Millennia (Spectra Physics). The Tsunami produces 728 nm laser pulses having a pulse duration of 50 fs, repetition rate of 80 MHz, and pulse energy of 8.5 nJ. The fundamental 728 nm beam was frequency doubled with a nonlinear crystal (1 mm BBO, $\theta = 25°$, $\phi = 90°$). The polarization of the second-harmonic excitation beam was rotated by a Berek compensator so as to collect the emission decay at magic angle polarization. To avoid possible photodegradation, the laser power was reduced to ~40 mW (0.5 nJ/pulse) by placing neutral density filters before the sample and the sample was placed in a rotating cell of path length 1 mm. The fluorescence emitted from the sample was upconverted in a nonlinear crystal (0.5 mm BBO, $\theta = 38°$, $\phi = 90°$) using a gate beam of 728 nm. The upconverted light was dispersed in a monochromator and detected using photon counting electronics. A cross-correlation function obtained using the Raman scattering from ethanol displayed a full width at half-maximum (fwhm) of 165 fs. The femtosecond fluorescence decays were fitted using SCIENTIST software.

3. Results and Discussion

3.1. Functionalization of $Au_{25}SG_{18}$ with Dansyl Chromophore. Dansyl chromophore was attached to the Au_{25} core by two different routes as mentioned above. In the first route, dansyl chloride was reacted at the amino group of the glutamate residue of some of the glutathione ligands (-SG) anchored on Au_{25}. This gives Au_{25} cluster protected with a mixture of glutathione and *N*-dansyl glutathione. The product obtained in this route is referred to as the *reaction product* in the ongoing discussion. In the second route, some of the glutathione ligands of the cluster underwent exchange by the classical ligand-exchange method with dansyl glutathione (-SG-D) when the $Au_{25}SG_{18}$ was stirred with dansyl glutathione. This method also led to the formation of Au_{25} protected with a mixture of glutathione and *N*-dansyl glutathione. The product obtained here is referred to as the *exchange product*. The dansyl-functionalized Au_{25} obtained through the two methods was characterized.

$Au_{25}SG_{18}$ has a well-structured optical absorption spectrum with an absorption maximum at 672 nm, and the absorption intensity increases toward the lower wavelength region. The peak at 672 nm (1.55 eV) arises due to a LUMO ← HOMO transition which can be called an intraband (sp ← sp) transition. The features in the lower wavelength region arise due to interband transition (sp ← d).[33,39] All the absorption features of Au_{25} in the visible and ultraviolet regions were seen in both the reaction and exchange products after repeated precipitation−purification cycles (Figure 1). Retention of the absorption profile after attachment of the chromophore confirms that the Au_{25} core is preserved. Due to the overlapping absorption features of the dansyl group and Au_{25}, the peaks due to the former are not distinct, although an increase in intensity at 323 nm due to the dansyl group is seen in D-GS-substituted Au_{25} samples. No free D-GSH or gold thiolate was seen in the solution, and the products were stable for weeks.

The products showed only faint spots due to the Au_{25} cores in high-resolution transmission electron microscopy as the core size is ~1 nm. Upon repeated electron beam exposure, the adjacent particles tend to fuse together, producing larger particles of 2 nm average diameter.[37] The presence of -SG-D groups on the cluster was confirmed by ESI-MS (Figure 2) and LDI-MS (Supporting Information 3), which showed features due to dansyl glutathione and the dansyl fragment at *m/z* 541 and 235,

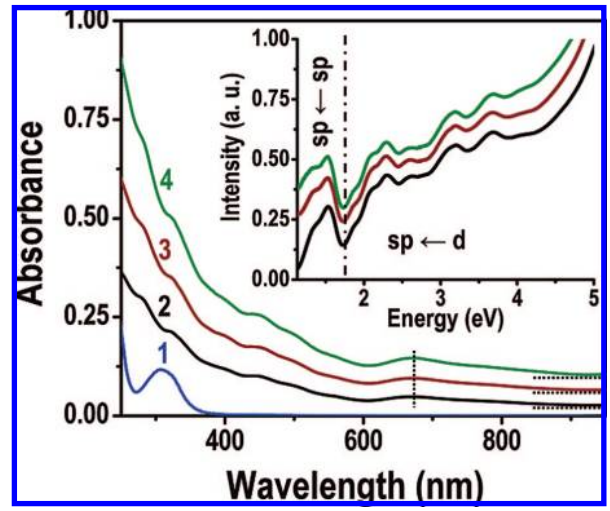

Figure 1. Comparison of the optical absorption features of (1) dansyl glutathione, (2) $Au_{25}SG_{18}$, (3) reaction product, and (4) exchange product. Au_{25} itself has an absorption feature around 320 nm which masks the dansyl peaks in the products. (Inset) Plot of $I(E) = A(W) \times W^2$ vs energy (eV). The characteristic absorption features of Au_{25} are retained in both the reaction and the exchange products, and the peak at 672 nm does not show any shift after dansyl functionalization. The spectra have been shifted vertically for clarity.

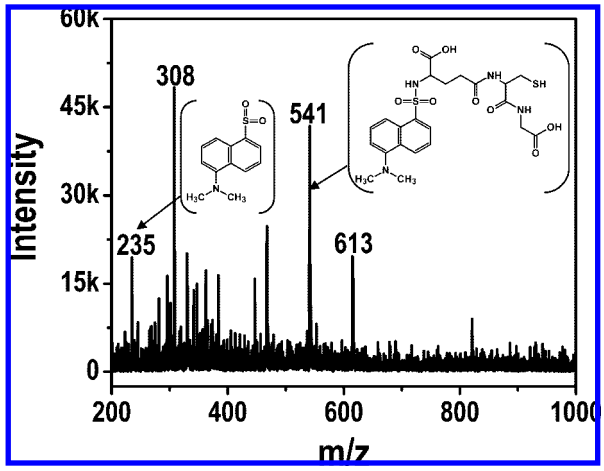

Figure 2. Positive-ion ESI-MS of the reaction product showing the features of dansyl glutathione (*m/z* 541), glutathione (*m/z* 308), dansyl group (*m/z* 235), and glutathione dimer (*m/z* 613). Molecular mass of dansyl glutathione is 540, and that of the dansyl fragment is 234 (the fragments are shown in the figure). ESI-MS (water:methanol 1:1, 20 ppm sample) shows the protonated ions. These features were seen in the exchange product also.

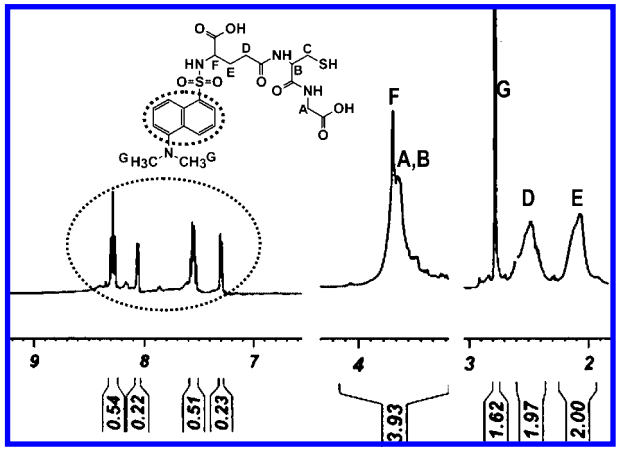

Figure 3. ^{1}H NMR spectrum of the dansyl-functionalized Au_{25} obtained through the reaction route. The peaks are labeled. ^{1}H NMR spectrum of pure $Au_{25}SG_{18}$ is given in Supporting Information 1c.

respectively. The features due to glutathione (*m/z* 308) and glutathione dimer (*m/z* 613) were also seen in the spectra. The ions mentioned above are the protonated species. Both the reaction and exchange products showed features due to the presence of the dansyl chromophore. These peaks are absent in parent $Au_{25}SG_{18}$. ESI-MS in the orthogonal geometry as in ours does not give features due to intact $Au_{25}SG_{18}$ as reported previously.[33]

Dansyl attachment can also be confirmed from the ^{1}H NMR spectrum of the dansyl-functionalized $Au_{25}SG_{18}$. The NMR spectrum of the reaction product (Figure 3) shows the features due to dansyl glutathione. The peaks are broadened due to the non-uniform distribution of ligands on the cluster surface and the dipolar spin relaxation of the ligand on the densely packed region near the thiolate/gold interface. The peaks in the NMR spectrum are labeled. The ^{1}H NMR of pure $Au_{25}SG_{18}$ is given in Supporting Information 1c, which shows features due to groups A, B, D, E, and F. The methylene (marked as C) close to the -SH broadens to the baseline in $Au_{25}(SG)_{18}$. This absence is understandable, which also confirms thiolate binding on the Au_{25} core. The peaks due to the naphthalene ring of the dansyl group which appear at higher ppm values are absent in the NMR

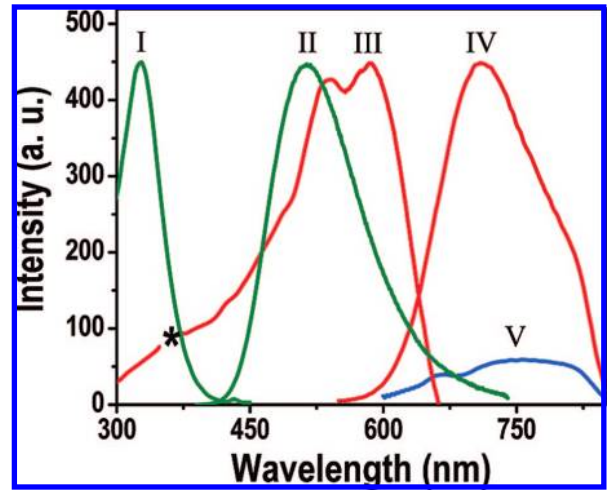

Figure 4. (I) Dansyl glutathione excitation, (II) dansyl glutathione emission, (III) Au_{25} excitation, and (IV and V) Au_{25} emissions at 535 and 330 nm excitations, respectively. The spectra are normalized with respect to the Au_{25} emission at 535 nm excitation. Significant overlap of the D-GSH emission and Au_{25} excitation indicates the possibility of energy transfer. Asterisk corresponds to the region at which a higher order line of the grating masks the spectrum. The apparent increase of the intensity of the peak at 585 nm in the excitation spectrum of Au_{25} compared to the peak at 535 nm is due to Jacobian correction.

spectrum of pure $Au_{25}SG_{18}$. The peaks due to the dansyl fragment are not broad in comparison to the glutathione portion. This is due to the distant location of the dansyl group from the Au_{25} core. To determine the number of dansyl glutathione per Au_{25} cluster, the NMR intensities of the aromatic resonances of the naphthalene ring of the dansyl group and those of the glutathione linker were integrated. The average ratio of glutathione and dansyl glutathione per cluster was found to be 3:1.

3.2. Photoluminescence of $Au_{25}SG_{18}$ and Dansyl Glutathione. Since $Au_{25}SG_{18}$ has molecule-like electronic structure, it exhibits photoluminescence. The origin of the emission is not clearly understood currently but can be attributed to the sp intraband excitation.[33] In the photoluminescence spectrum, the cluster shows an excitation maximum at 535 nm and an emission maximum at 700 nm. The cluster also shows a weak emission when excited in the UV region. The excitation profile of the cluster is different from the absorption profile. The peak at 672 nm, observed in the absorption spectrum, is not present in the excitation profile as reported earlier.[33] The excitation spectrum of $Au_{25}SG_{18}$ shows some difference in the 300−600 nm region compared to that reported,[33] and to check this, spectra from various instruments were measured (Supporting Information 4). There are minor differences between the spectra that are attributed to detector efficiencies. The quantum yield of the cluster is 1.9×10^{-3}, which is very high compared to bulk gold. Synthesized dansyl glutathione shows excitation and emission at 323 and 505 nm, respectively. Since the emission spectrum of dansyl glutathione overlaps with the excitation spectrum of Au_{25}, there is a possibility of fluorescence resonance energy transfer (FRET) between them. Figure 4 depicts the excitation and emission profiles of the dansyl glutathione (D-GSH), the donor, and $Au_{25}SG_{18}$, the acceptor.

3.3. Energy Transfer between the Dansyl Chromophore and $Au_{25}SG_{18}$. Steady-state fluorescence measurements were carried out on both the exchange and reaction products in order to check whether any energy transfer occurred between the cluster and the chromophore. It was found that emission of dansyl glutathione underwent drastic quenching in both products. Figure 5 depicts the emission profile of the reaction product.

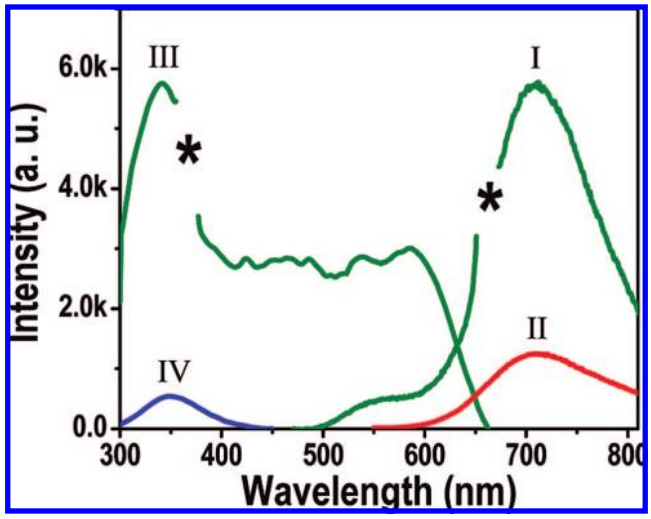

Figure 5. Steady-state fluorescence spectra of the reaction product. (I and II) Emission spectra obtained when excited at 330 and 535 nm, respectively, showing the same emission maximum. (III and IV) Corresponding excitation spectra for emission at 700 and 550 nm. The emission at 550 nm is the quenched donor emission. Asterisks correspond to regions where higher order lines of the grating mask the spectrum.

The quenching of the donor is seen clearly. On the other hand, the emission at 700 nm, which is the characteristic emission of Au_{25}, was enhanced in both the reaction and the exchange products when excited at the excitation maximum of the donor (330 nm). It is clear from Figure 5 that the intensity of the emission collected when excited at 535 nm (excitation maximum for the parent Au_{25}) is low when compared with the emission collected at 350 nm excitation. This clearly establishes energy transfer from the dansyl chromophore to Au_{25}. The emission profile of the exchange product is given in Supporting Information 5. Our earlier report on functionalization of Au_{25} with different ligands like *N*-acetyl and *N*-formyl glutathione showed that ligand exchange of glutathione of $Au_{25}SG_{18}$ with its derivatives does not change the emission profile.[37] Both the *N*-acetyl and *N*-formyl glutathione-functionalized Au_{25} showed the same excitation and emission maxima as that of parent Au_{25}. From this it can be concluded that mere ligand exchange with glutathione derivatives does not alter the photoluminescence profile. However, energy transfer occurred between dansyl chromophore and Au_{25}.

3.4. Femtosecond Time-Resolved Study. From the lifetime measurements, a faster decay of fluorescence is observed in both dansylated products compared to the parent donor (Figure 6). The decay is faster for the exchange product than the reaction product. Note that the chromophore underwent complete quenching in the case of exchange product (Supporting Information 5) and hence faster decay. From multiexponential fitting of the fluorescence transient of the donor, time constants of 0.85 (29.6%), 6.40 (42.9%), and 39.05 ps (27.5%) were obtained. The time constants are consistent with the reported study on the ultrafast deactivation pathways of the dansyl fluorophore in bulk methanol.[41] The femtosecond-resolved study on the dansyl chromophore reveals that the subpicosecond component is due to the ultrafast solvation dynamics in polar environments (water in our case), and other two components are associated with the structural relaxation of the probe. The excited-state lifetime of the probe, which is reported to be 9−12 ns reflected in the offset in the fluorescence decay, does not decay reasonably in our experimental window of 4 ps. The overall average lifetime of the probe of 13.75 ps is also consistent with the previous

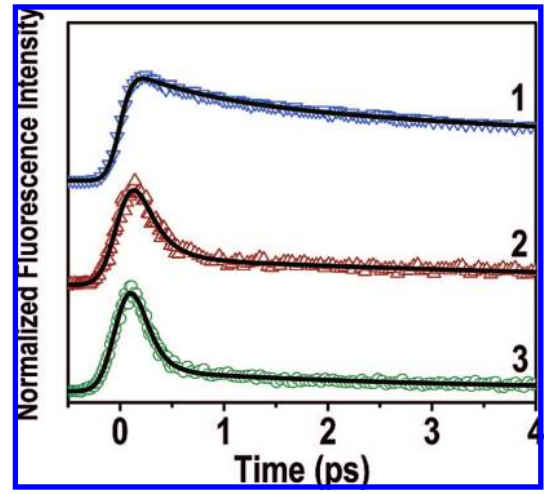

Figure 6. Femtosecond time-resolved fluorescence transients of (1) D-GSH, (2) reaction, and (3) exchange products. The samples were excited at 364 nm, and the transients were collected at 500 nm.

report.[41] However, in the case of the donor−acceptor systems, much shorter components of 0.20 (86.8%) and 5.10 ps (13.2%) for the reaction product and 0.15 (92.4%) and 3.00 ps (7.6%) for the exchange product are observed. The overall lifetimes of the probe in the presence of acceptor Au_{25} (0.85 ps for reaction product and 0.35 ps for exchange product) reveal significant fluorescence quenching compared to that in the donor (13.75 ps). This indicates that large nonradiative resonance energy transfer has taken place from the dansyl chromophore to Au_{25}. The significant quenching of the donor fluorescence along with the shorter excited-state lifetime of the donor as a consequence of D−A dipolar coupling confirms the FRET mechanism. Since the percentage of dansyl glutathione per cluster is only 25, they are expected to be far apart due to steric effects, and hence, the dipole−dipole coupling within D−D pairs would be negligible. The energy-transfer efficiency and distance between the dansyl chromophore and the metal cluster in dansylated-Au_{25} are determined using the FRET technique.

3.4.1. Förster's Resonance Energy Transfer Technique. In order to estimate the Förster's resonance energy-transfer efficiency of the donor (D-GSH) and hence determine distances of donor−acceptor pairs, we followed the methodology described in chapter 13 of ref 42. The Förster distance (d_0) is given by

$$d_0 = 0.211[\kappa^2 n^{-4} Q_D J(\lambda)]^{1/6} \quad (\text{in Å})$$

where κ^2 is a factor describing the relative orientation in space of the transition dipoles of the donor and acceptor. For donor and acceptors that randomize by rotational diffusion prior to energy transfer, the magnitude of κ^2 is assumed to be 2/3. The refractive index (n) of the aqueous medium is assumed to be 1.33. In order to determine the quantum yield (Q_D) of the donor, proflavin in water (pH = 7) with a quantum yield of 0.34 has been used as the standard.[43] The quantum yield of the D-GSH is found to be 0.129 in the absence of acceptor. $J(\lambda)$, the overlap integral, which expresses the degree of spectral overlap between the donor emission and the acceptor absorption, is given by

$$J(\lambda) = \frac{\int_0^\infty F_D(\lambda)\varepsilon(\lambda)\lambda^4 \, d\lambda}{\int_0^\infty F_D(\lambda) \, d\lambda}$$

where $F_D(\lambda)$ is the fluorescence intensity of the donor in the wavelength range from λ to $\lambda + d\lambda$ and is dimensionless. $\varepsilon(\lambda)$

is the extinction coefficient (in M^{-1} cm^{-1}) of the acceptor at λ. Here, ε is taken to be 8800 M^{-1} cm^{-1} at 670 nm.[33] If λ is in nm, then $J(\lambda)$ is in units of M^{-1} cm^{-1} nm^4. Once the value of R_0 is known, the donor−acceptor distance (d) can be calculated using the formula

$$d^6 = [d_0^6(1 - E)/E]$$

Here E is the efficiency of energy transfer. The transfer efficiency is measured using the average lifetime of the donor in the absence (τ_D) and presence (τ_{DA}) of the acceptor. The efficiency E is calculated from the lifetimes using the following equation

$$E = 1 - \frac{\tau_{DA}}{\tau_D}$$

The donor−acceptor distance was determined using the above equations. The overlap integral [$J(\lambda)$] and Förster radius (d_0) are determined to be 1.91 × 10^{15} M^{-1} cm^{-1} nm^4 and 41 Å, respectively. The donor−acceptor separations (d) for the reaction and exchange products are 25.9 and 22.2 Å, respectively. This corresponds to a very high efficiency of energy transfer. The theoretically estimated distance between the Au_{25} cluster and the dansyl chromophore (center to center), assuming standard bond lengths, is around 23 Å, which matches with the experimental data.

3.4.2. Nanosurface Energy-Transfer Technique. The D−A separations can also be calculated using another prevailing technique, nanosurface energy transfer (NSET),[20,44] in which the energy-transfer efficiency depends on the inverse of the fourth power of the donor−acceptor separation. The nanosurface energy-transfer technique is based on the model of Persson and Lang,[44] which is concerned with the momentum and energy conservation in the dipole-induced formation of electron−hole pairs. Here the rate of energy transfer is calculated by performing a Fermi golden rule calculation for an excited-state molecule depopulating with the simultaneous scattering of an electron in the nearby metal to above the Fermi level. The Persson model states that the damping rate to a surface of a noble metal may be calculated by

$$k_{et} = 0.3\left(\frac{\mu^2\omega_{dye}}{\eta\omega_F k_F d^4}\right)$$

which can be expressed in more measurable parameters through the use of the Einstein A_{21} coefficient[45]

$$A_{21} = \frac{\omega_{dye}^3}{3\varepsilon_0\eta\pi c^3}|\mu|^2$$

To give the following rate of energy transfer in accordance with Coulomb's law ($1/4\pi\varepsilon_0$)

$$k_{et} = 0.225\frac{c^3\Phi_{dye}}{\omega_{dye}^2\omega_F k_F d^4\tau_{dye}}$$

where c is the speed of light, ϕ_{dye} is the quantum yield of the donor (dansyl = 0.129), ω_{dye} is the angular frequency for the donor (5.71 × 10^{15} s^{-1}), ω_F is the angular frequency for bulk gold (8.4 × 10^{15} s^{-1}), d is the donor−acceptor separation, τ_{dye} is the average lifetime of the dye (13.75 ps), and k_F is the Fermi wavevector for bulk gold (1.2 × 10^8 cm^{-1}). The d_0 value is a convenient value to calculate for a dye−metal system, yielding the distance at which a dye will display equal probabilities for energy transfer and spontaneous emission. For the Persson model the d_0 value may be calculated by

$$d_0 = \left(0.225\frac{c^3\Phi_{dye}}{\omega_{dye}^2\omega_F k_F}\right)^{1/4}$$

In our case we used $k_{time\text{-}resolved}$ as k_{et}

$$k_{time\text{-}resolved} = \frac{1}{\tau_{donor\text{-}acceptor}} - \frac{1}{\tau_{dye}}$$

where $\tau_{donor-acceptor}$ is the average lifetime of the donor−acceptor system. The calculated D−A values using NSET are 19.9 and 15.8 Å for the reaction and exchange products, respectively. The results obtained are summarized in Table 1. In either case, the shorter D−A separation for the exchange product is because during exchange some of the glutathione ligands attached to the cluster are removed and dansyl glutathione occupies the space provided with the dansyl group projecting toward the liquid phase. In the reaction product, dansylation is carried out directly on the assembly of glutathione ligands on the cluster surface. Due to steric hindrance, reaction occurs only on those ligands which are farthest from the core and hence a longer D−A distance. In either case, the data reflect the asymmetry in the ligand binding on the metal core, supporting the structures proposed using experiment[46] and theory.[47]

TABLE 1: Summarized Data of Energy Transfer

sample	average lifetime (ps)	$k_{time\text{-}resolved}$	NSET		FRET	
			d_0 (Å)	d (Å)	d_0 (Å)	d (Å)
dansyl glutathione	13.75		39.3		40.8	
reaction product	0.85	1.1×10^{12}		19.9		25.9
exchange product	0.35	2.8×10^{12}		15.8		22.2

4. Conclusion

We demonstrated very efficient FRET between the molecular gold cluster, Au_{25}, and the dansyl chromophore. The cluster was functionalized by two different routes, and in both cases a drastic quenching of the donor's emission was observed. Accurate determination of the distance between the chromophore and the metal core suggests inhomogeneous ligand binding on the cluster. The results reflect the asymmetry in the ligand binding on the metal core of Au_{25}, supporting the structures proposed using experiment and theory. It is possible to use the system for biological and other purposes. This is especially useful in the context of biocompatibility of gold.

Acknowledgment. We thank the Department of Science and Technology (DST), Government of India, for constantly supporting our research program on nanomaterials.

Supporting Information Available: UV−vis, FT-IR, and FT-NMR of $Au_{25}SG_{18}$; excitation and emission spectra and ESI-MS of dansyl glutathione; excitation and emission spectra of $Au_{25}SG_{18}$ collected from various instruments, LDI-MS of reaction product, and steady-state photoluminescence profile of the exchange product. This material is available free of charge via the Internet at http://pubs.acs.org.

References and Notes

(1) Hass, E. *Protein Folding Handbook*; Buchner, J., Kiefhaber, T., Eds.;WILEY-VCH: Weinheim, Germany, 2005: Vol. 2, pp 573−633.

(2) Ray, P. C.; Fortner, A.; Darbha, G. K. *J. Phys. Chem. B* **2006**, *110*, 20745.

(3) Qiang, M.; Xing-Guang, S.; Xin-Yan, W.; Yi, W.; Chun-Lei, W.; Bai, Y.; Qin-Han, J. *Talanta* **2005**, *67*, 1029.
(4) Zhang, J.; Fu, Y.; Lakowicz, J. R. *J. Phys. Chem. C* **2007**, *111*, 50.
(5) Bagalkot, V.; Zhang, L.; Levy-Nissenbaum, E.; Jon, S.; Kantoff, P. W.; Langer, R.; Farokhzad, O. C. *Nano Lett.* **2007**, *7*, 3065.
(6) Shi, L.; De Paoli, V.; Rosenzweig, N.; Rosenzweig, Z. *J. Am. Chem. Soc.* **2006**, *128*, 10378.
(7) Tang, Z.; Ozturk, B.; Wang, Y.; Kotov, N. A. *J. Phys. Chem. B* **2004**, *108*, 6927.
(8) Wargnier, R.; Baranov, A. V.; Maslov, V. G.; Stsiapura, V.; Artemyev, M.; Pluot, M.; Sukhanova, A.; Nabiev, I. *Nano Lett.* **2004**, *4*, 451.
(9) Muller, F.; Gotzinger, S.; Gaponik, N.; Weller, H.; Mlynek, J.; Benson, O. *J. Phys. Chem. B* **2004**, *108*, 14527.
(10) Ebenstein, Y.; Mokari, T.; Banin, U. *J. Phys. Chem. B* **2004**, *108*, 93.
(11) Sarkar, R.; Narayanan, S. S.; Palsson, L.-O.; Dias, F.; Monkman, A.; Pal, S. K. *J. Phys. Chem. B* **2007**, *111*, 12294.
(12) Shi, L.; Rosenzweig, N.; Rosenzweig, Z. *Anal. Chem.* **2007**, *79*, 208.
(13) Narayanan, S. S.; Pal, S. K. *J. Phys. Chem. B* **2006**, *110*, 24403.
(14) Bagalkot, V.; Zhang, L.; Levy-Nissenbaum, E.; Jon, S.; Kantoff, P. W.; Langer, R.; Farokhzad, O. C. *Nano Lett.* **2007**, *7*, 3065.
(15) Ray, P. C.; Darbha, G. K.; Ray, A.; Walker, J.; Hardy, W. *Plasmonics* **2007**, *2*, 173.
(16) Watanabe, J.; Ishihara, K. *Bioconjugate Chem.* **2007**, *18*, 1811.
(17) Oh, E.; Hong, M.-Y.; Lee, D.; Nam, S.-H.; Yoon, H. C.; Kim, H.-S. *J. Am. Chem. Soc.* **2005**, *127*, 3270.
(18) Darbha, G. K.; Anandhi, R. A.; Ray, P. C. *ACS Nano* **2007**, *1*, 208.
(19) Jennings, T. L.; Singh, M. P.; Strouse, G. F. *J. Am. Chem. Soc.* **2006**, *128*, 5462.
(20) Montalti, M.; Zaccheroni, N.; Prodi, L.; O'Reilly, N.; James, S. L. *J. Am. Chem. Soc.* **2007**, *129*, 2418.
(21) Seelig, J.; Leslie, K.; Renn, A.; Kuhn, S.; Jacobsen, V.; van de Corput, M.; Wyman, C.; Sandoghdar, V. *Nano Lett.* **2007**, *7*, 685.
(22) Li, H.; Rothberg, L. J. *Anal. Chem.* **2004**, *76*, 5414.
(23) Jinlong, C.; AiFang, Z.; AiHong, C.; Yingchun, G.; Chiyang, H.; Xiaoming, K.; Genhua, W.; Youcun, C. *Anal. Chim. Acta* **2007**, *599*, 134.
(24) Chen, S.-J.; Chang, H.-T. *Anal. Chem.* **2004**, *76*, 3727.
(25) Zhu, L.; Wu, W.; Zhu, M.-Q.; Han, J. J.; Hurst, J. K.; Li, A. D. Q. *J. Am. Chem. Soc.* **2007**, *129*, 3524.
(26) Hong, S. W.; Ahn, C.-H.; Huh, J.; Jo, W. H. *Macromolecules* **2006**, *39*, 7694.
(27) Kong, H. J.; Kim, C. J.; Huebsch, N.; Weitz, D.; Mooney, D. J. *J. Am. Chem. Soc.* **2007**, *129*, 4518.
(28) Duan, H.; Nie, S. *J. Am. Chem. Soc.* **2007**, *129*, 2412.
(29) Zheng, J.; Nicovich, P. R.; Dickson, R. M. *Annu. Rev. Phys. Chem.* **2007**, *58*, 409.
(30) Zheng, J.; Petty, J. T.; Dickson, R. M. *J. Am. Chem. Soc.* **2003**, *125*, 7780.
(31) Zheng, J.; Zhang, C. W.; Dickson, R. M. *Phys. Rev. Lett.* **2004**, *93*, 077402.
(32) Schaaff, T. G.; Knight, G.; Shafigullin, M. N.; Borkman, R. F.; Whetten, R. L. *J. Phys. Chem. B* **1998**, *102*, 10643.
(33) Negishi, Y.; Nobusada, K.; Tsukuda, T. *J. Am. Chem. Soc.* **2005**, *127*, 5261.
(34) Shichibu, Y.; Negishi, Y.; Tsukuda, T.; Teranishi, T. *J. Am. Chem. Soc.* **2005**, *127*, 13464.
(35) Shichibu, Y.; Negishi, Y.; Tsunoyama, H.; Kanehara, M.; Teranishi, T.; Tsukuda, T. *Small* **2007**, *3*, 835.
(36) Habeeb Muhammed, M. A.; Pradeep, T. *Chem. Phys. Lett.* **2007**, *449*, 186.
(37) Shibu, E. S.; Habeeb Muhammed, M. A.; Tsukuda, T.; Pradeep, T. *J. Phys. Chem C*, in press.
(38) Zhu, M.; Lanni, E.; Garg, N.; Bier, M. E.; Jin, R. *J. Am. Chem. Soc.* **2008**, *130*, 1138.
(39) Zhu, M.; Aikens, C. M.; Hollander, F. J.; Schatz, G. C.; Jin, R. *J. Am. Chem. Soc.* **2008**, *130*, 5883.
(40) Gan, J.; Harper, T. W.; Hsueh, M.-M.; Qu, Q.; Humphreys, W. J. *Chem. Res. Toxicol.* **2005**, *18*, 896.
(41) Zhong, D.; Pal, S. K.; Zewail, A. H. *Chem. Phys. Chem.* **2001**, *2*, 219.
(42) Lakowicz, J. R. *Principles of Fluorescence Spectroscopy*; Kluwer Academic/Plenum: New York, 1999.
(43) Melhuish, W. H. *J. Opt. Soc. Am.* **1964**, *54*, 183.
(44) Persson, B. N. J.; Lang, N. D. *Phys. Rev. B* **1982**, *26*, 5409.
(45) Craig, D.; Thirunamachandran, T. *Molecular Quantum Electrodynamics*; Academic Press: London, 1984.
(46) Heaven, M. W.; Dass, A.; White, P. S.; Holt, K. M.; Murray, R. W. *J. Am. Chem. Soc.* **2008**, *130*, 3754.
(47) Akola, J.; Walter, M.; Whetten, R. L.; Hakkinen, H.; Gronbeck, H. *J. Am. Chem. Soc.* **2008**, *130*, 3756.

JP804597R